

lar, providing generative models with more versatile applications. In particular, Vidu [48] and PIKA[32] have introduced multi-subject reference video generation models, which have had a significant impact on social media. Thus, there is growing interest in subject-centric generation, where models focus solely on generating the primary subject while excluding background or contextual elements.

Current AI-generated models [7, 11, 19, 33, 38, 40] can produce visually impressive results. However, they often lack structural decomposition and layer-wise editability, which are essential for seamless integration into professional design workflows. The core challenge lies in bridging the gap between image generation and real visual-content-creation workflow requirements. Users need AI tools that not only produce high-quality outputs, but also support element-level control, flexible recomposition, and natural blending with existing design contexts.

One possible solution is RGBA image generation. For example, [51] constructed a dataset of one million images with transparency channels and used it to train a diffusion model capable of generating images with transparency. While this method enables the generation of RGBA images that can be applied in certain contexts, it requires a substantial amount of training data. Additionally, the generated images often exhibit continuous alpha channel values, which may not be necessary for many practical applications. Through extensive industry surveys, we found that in many practical applications—such as T-shirt prints, stickers, and logos—a continuous alpha channel is not required. Instead, these applications typically need distinct, discrete alpha values for clear separation of objects from the background, making the use of continuous alpha channel values less suitable and potentially introducing unnecessary complexity.

To bridge this gap, a prevalent solution adopts a two-stage generation-then-segmentation paradigm. In the first stage, advanced image generation models like [19] produce high-quality synthetic images. These outputs are then processed through segmentation modules, where universal segmentation frameworks such as SAM [18] can parse all image elements, while salient object detectors like [12] focus on extracting primary subjects. However, this approach often requires expert knowledge and the integration of multiple models, which can complicate the process and reduce its accessibility.

To improve the practical value of AI-generated images in visual content creation, it is essential to address the challenges of subject-centric images generation and ensuring the effective integration of elements. In response to these needs, we propose a novel image generation pipeline that seamlessly integrates with advanced generative models. In this work, we leverage the state-of-the-art pre-trained text-to-image model, such as FLUX [19], to generate the visual

elements. Many researches has proven that it is effective to condition diffusion model by manipulating cross-attention or self-attention layers [6, 9, 13, 47], indicating that cross-attention maps convey valuable information [45]. Based on this insight, we propose an entropy-based feature fusion strategy to integrate attention maps linked to the most influential prompt words (typically nouns related to the foreground) during each sampling step. This approach enhances the fidelity of detecting salient element in image generation process by strategically manipulating attention features. Moreover, the formulation and selection of prompts have a significant impact on our results. To make the entire process feasible and automated, we design an agent framework, which allows us to obtain richly detailed results by simply input desired elements and style while automatically selecting key elements to guide the subject-centric image generation.

Finally, our method produces faithful image generation results that can be seamlessly adapted to a wide range of industrial applications, from merchandise printing to digital media, ensuring smooth integration with diverse background patterns and ready for real-world production.

The workflow most similar to ours combines generation with salient object detection (SOD) [4]. We have compared our approach with SAM[18] and its derivatives for SOD[12], as well as with the generation-then-matting method[35, 54]. Additionally, we conducted comparisons with RGBA-based generation techniques [37, 51] to assess their performance and suitability for our application. Extensive experimental results suggest that our method offers greater reliability. This advantage arises from our ability to generate high-quality images while ensuring the precise creation of key elements, indicating that our approach is well-suited for creative applications.

In summary, our contribution can be organized as follows:

- We have developed a zero-shot subject-centric generative approach, which is capable of generating images with accurate synthesis of primary subject, outperforming existing methods.
- We proposed an entropy-based feature fusion module which leverages the informative cross-attention feature map of the diffusion reverse steps, enabling us to accurately retain the chosen elements.
- We designed an agent based on large language models that extends users' simple and casual input into more expressive prompts while extracting primary elements, filtering out irrelevant objects, greatly enhancing the accuracy of primary elements synthesis.
- Experimental results demonstrate that our approach has achieve SOTA performance in subject-centric generation, and ablation studies show the effectiveness of our designed components. The code will be release publicly to

facilitate future research.

2. Related Work

Diffusion Models. Originated from Diffusion Probabilistic Model [43], diffusion models began to receive widespread attention when researchers proposed practical training and sampling algorithms [15, 28, 44]. Furthermore, [10, 31] proposed Diffusion Transformers, which replace the convolutional U-Net structure with transformers, enhancing the scalability and visual quality of diffusion models. These above works have paved the way for recent large-scale diffusion models like Stable Diffusion [33, 38] and Flux [19]. There are many works which try to enhance the controllability of the generated image from large-scale diffusion models. One approach is to develop effective fine-tuning methods based on additional guidance information, such as ControlNet [52], T2I-adapter [27]. Another approach is to exploit the zero-shot capabilities of pre-trained diffusion models by proposing tuning-free methods to change the denoising process. Many of them are based on the manipulation of cross-attention or self-attention layers [6, 9, 13, 47]. Some in-depth discussions about the role of cross and self-attention layers in stable diffusion are provided in [22].

Subject-Centric Generation. Conventional subject-centric creation workflows typically decouple content generation from element extraction. A key challenge in such cascaded frameworks is error accumulation: segmentation accuracy is inherently tied to generation quality, while post-processing techniques, such as segmentation [18] and SOD [12], often struggle with fine details, leading to imprecise boundaries and missing intricate structures. Additionally, alpha estimation using matting methods [36, 50] can introduce artifacts that are incompatible with standard constraints—particularly the requirement for a binary alpha channel, necessitating an additional thresholding step, which may further degrade edge fidelity.

Recent efforts attempt tighter integration: LayerDiffusion [20] fine-tunes foundation models for transparency generation, while Alfie [37] modifies diffusion attention mechanisms for RGBA output. However, these methods often struggle with strict alpha compositing constraints, leading to inconsistencies when integrating with standard design pipelines. Additionally, RGBA-based approaches inherently suffer from color bleeding, edge inconsistencies, and difficulty in achieving precise subject-centric generation.

Prompt Engineering. With the growing popularity of text-to-image models, researchers focus on the impact of text on the quality of image generation. Some researchers [23] explore the text design in text-to-image generative models and systematically summarize them into design guidelines to achieve better image quality. 3DALL-E [24] tried using GPT-3 to rewrite selected prompts. Prompt-to-prompt

[14] proposes an editing framework that can semantically edit images by modifying prompts in a pre-trained text-conditional diffusion model. Promptify [5] is based on a large language model and helps users improve original text prompts through a visual interface and interactive system. Omnost [46] enhance image generation and user-friendliness by optimizing user input prompts and selecting the most appropriate generation model.

Our work is the first attempt to explore prompt optimization by the agent and build an agent framework for prompt expansion and key elements extraction, which can enhance attention map extraction and RGBA image generation.

3. Methods

In this section, we propose a zero-shot method to synthesize images where the primary subject is accurately generated while minimizing the presence of extraneous elements. Additionally, we introduce an agent-based framework that simplifies user input by automatically structuring it into an optimized format for subject generation, reducing the need for manual intervention. We begin with an introduction of overall framework (Sec. 3.1) and then introduce rectified flow and MM-DiT architecture (Sec. 3.2) which are applied in FLUX model, next we propose our main contribution: Entropy-based Attention Weighting (Sec. 3.3) and Agent framework (Sec. 3.4).

3.1. Overview

As illustrated in Fig. 2, a fully automated framework is proposed for subject-centric generation: (1) Our method receives elements input by the user (*e.g.*, *Christmas, Santa, Tree*), utilizes an agent based on LLMs to automatically expand these elements into an expressive prompt, and extracts nouns related to primary elements (*e.g.*, **Christmas, Bells, Stars** *etc.*). (2) The expanded prompt is used for the conditional generation of the pre-trained text-to-image model Flux, producing three-channel RGB images denoted as $\hat{I} \in \mathcal{R}^{H \times W \times 3}$, where H and W defines the height and width of the image \hat{I} . Concurrently, in each diffusion reverse step t , we use keywords to index corresponding parts of each cross-attention map, which are then integrated using our proposed entropy-based weighting strategy. (3) We apply the merged cross-attention map as guidance to precisely predict the mask of the primary subject $M \in \mathcal{R}^{H \times W \times 1}$ that selectively removing irrelevant objects and preserving primary elements.

3.2. Diffusion Model

Conditional Rectified Flow Recent advancements in text-to-image generation are moving towards using rectified flow [3, 25] to construct an ordinary differential equation (ODE) that transports between two empirically observed distributions, x_0 and x_1 . In an ODE-based diffusion model, the

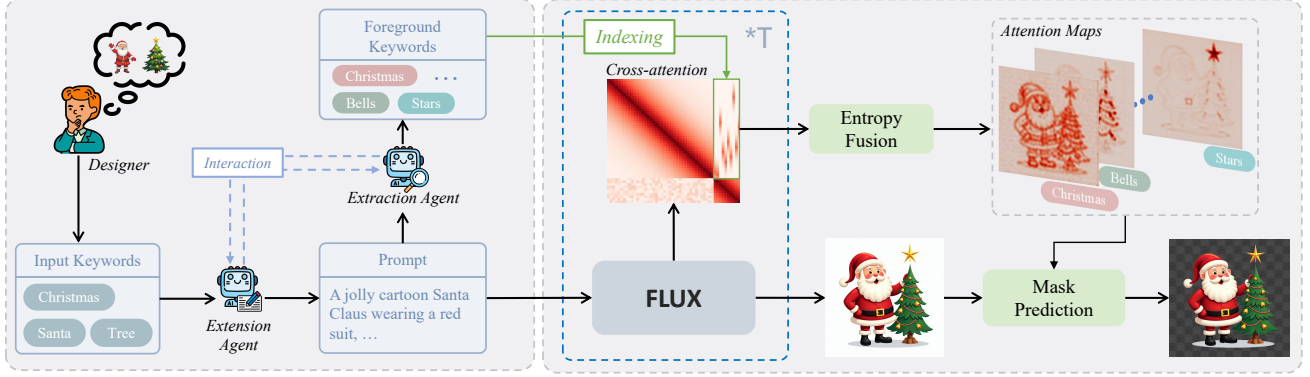


Figure 2. The overview of our pipeline includes agents responsible for prompt extension and keyword extraction. The prompt serves as the input for the pretrained FLUX model, while the extracted keywords guide the alpha channel estimation using an entropy-based feature fusion strategy, ultimately facilitating the RGBA image generation process.

evolution process is specified to follow the ODE: $\frac{dx}{dt} = f(x, t)$. Here, the focus is on approximating $\frac{dx}{dt}$ by a model $v_\theta(x, t)$ with trainable parameters θ , which represents the velocity at which x_0 evolves towards x_1 . As a simple example, let us assume the evolution from x_0 to x_1 is a straight line, especially when x_1 follows the standard distribution, we have:

$$x_t = (1 - t)x_0 + t\epsilon, \quad \text{where } \epsilon \sim \mathcal{N}(0, I). \quad (1)$$

Moreover, [11, 21] construct a conditional vector filled $u_t(x | \epsilon)$ which corresponds to a target probability density path $p_t(x | \epsilon)$. In such a way, it provides a objective known as Conditional Flow Matching (CFM):

$$\mathcal{L}_{CFM} = \mathbb{E}_{t, p_t(x|\epsilon), p(\epsilon)} \|v_\theta(x, t) - u_t(x | \epsilon)\|_2^2. \quad (2)$$

MM-DiT To construct $v_\Theta(x, t)$, the previously popular combination of UNet and Transformer models commonly used in diffusion models is increasingly being replaced by the DiT (Diffusion Transformer) architecture [30]. Recently, numerous models have adopted this approach, achieving notable results [1, 2, 19].

In order to better align text information with image information, MM-DiT does not directly apply cross-attention between the extracted text features and the features of each image layer as in many previous methods [33, 38]. Instead, it designs a dual-stream model: different trainable layers are assigned to different data modalities, and then they are concatenated for the attention operation. Recent studies [1, 2, 19] has proven that the MM-DiT architecture is effective for text-to-image generation. In our work, we utilize and explore the latest MM-DiT-based text-to-image pre-trained model, Flux [19].

3.3. Attention Extraction and Entropy-based Attention Weighing

Differ from previous pretrained text-to-image diffusion model [7, 33, 38], where cross-attention and self-attention are applied at different layers, Flux operates differently. It contains 19 dual-stream MM-DiT blocks and 38 single-stream DiT blocks. In dual-stream blocks, the image feature z and text embeddings e are processed separately, through different linear, scaling, and normalization layers. Afterward, they are concatenated and passed through the attention operation. In single-stream blocks, the image feature z and text embeddings are processed by the same transformers.

Since for each attention layer l , the image feature z and the text feature e are concatenated together for attention operation, the same strategy is applied consistently across all attention maps. Moreover, the attention map can be considered as a combination of the self-attention map and the cross-attention map. Similar to [37, 45], we specifically extract the cross-attention map to highlight the influence of key words. Formally, for a specific t and l , the attention map is defined as $\mathcal{A}_S^{t,l} \in \mathbb{R}^{(hw+N) \times (hw+N) \times f}$, where h and w represent the latent spatial dimensions, N represents the length of the text tokens, and f defines the number of feature channels.

$$\mathcal{A}_S^{t,l} := \text{softmax}(Q_{cat(z,e)}K_{cat(z,e)}/\sqrt{d}), \quad (3)$$

where \sqrt{d} stands for the scaling factor. Finally, the cross-attention $\mathcal{A}_C^{t,l} \in \mathbb{R}^{N \times hw \times C}$ can then extracted from $\mathcal{A}_S^{t,l}$ (see Fig. 2):

$$\mathcal{A}_C^{t,l} := \mathcal{A}_S^{t,l}[N :, : N, :]. \quad (4)$$

We observe that the information content in the cross-attention maps is not equal across different time steps and different layers. A simple accumulation might lead to sub-optimal subject mask estimation. This is due to the unequal

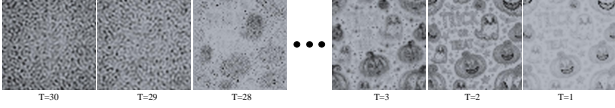


Figure 3. Illustration of the attention map of the FLUX model for the generation process with the prompt "trick or treat" across different denoising steps. We use the Euler distance sampling method. The results show that at different timesteps, the noise contains varying amounts of information.

contribution of information from each time step and layer, potentially diluting more informative features (see Fig. 3). Thus, we proposed an entropy-based attention map weighting strategy, assessing the information content of attention maps at different time steps and layers, which allows to assign greater weights to more informative maps during the weighting process. Specifically, for a given time t , layer l , and text token n 's attention map $\mathcal{A}_C^{t,l,n}$, we calculate its Histogram Probability $P_{t,l,n}$, then the entropy $H_{t,l}$ of $\mathcal{A}_C^{t,l,n}$ can be obtained as follows:

$$H_{t,l} = \frac{1}{N} \sum_{n=1}^N (-P_{t,l,n} \log_2 P_{t,l,n}). \quad (5)$$

Ultimately, we can perform weighting on each attention map $\mathcal{A}_C^{t,l}$ across all T steps and all L layers:

$$W_{\mathcal{A}_C^{t,l}} = \frac{1}{H_{t,l} + 1e - 6}, \quad (6)$$

$$\mathcal{A}_C = \frac{1}{TL} \sum_{l=1}^L \sum_{t=1}^T W_{\mathcal{A}_C^{t,l}} \times \mathcal{A}_C^{t,l}. \quad (7)$$

Through this method, we can obtain the cross-attention map \mathcal{A}_C corresponding to prompt e . We then select primary elements $\hat{n}_{fg} = [\hat{n}_1, \dots, \hat{n}_{\hat{N}}]$ and extract their associated attention maps $\mathcal{A}_C^{\hat{n}_{fg}}$ from \mathcal{A}_C to guide alpha estimation. Finally, these attention maps are organized into a 4-value map, which is then used in GrabCut[39] to guide the subject segmentation. As illustrated in Fig. 3, we visualized the cross-attention maps produced by two fusion strategies: standard addition and entropy-weighting. The resulting attention maps for each keyword and final generated images demonstrate that using an entropy-weighting strategy yields a clearer cross-attention map with reduced noise influence.

We observe that the highlighted regions in the feature map are strongly associated with the word, which impacts the accuracy of our decision on which object to retain. Words irrelevant to primary elements can affect the accuracy of alpha channel estimation. To optimize prompt composition and keyword extraction for primary elements, we introduce an agent framework to address this challenge.

3.4. Agent-based prompt extension and keywords extraction

To enhance the effect of our approach on subject-centric generation, we propose an agent-driven framework, which can output higher quality prompt and elements through reflection [42] and multi-agent collaboration. The framework extends key elements or casual user input K into a detailed scene prompt \hat{P} with enriched elements for image generation, then extracts primary elements \hat{n}_{fg} from the prompt to enable accurate extraction of the required attention map $\mathcal{A}_C^{\hat{n}_{fg}}$. The whole framework is illustrated in Alg. 1.

Algorithm 1 The algorithm of multi-agent framework.

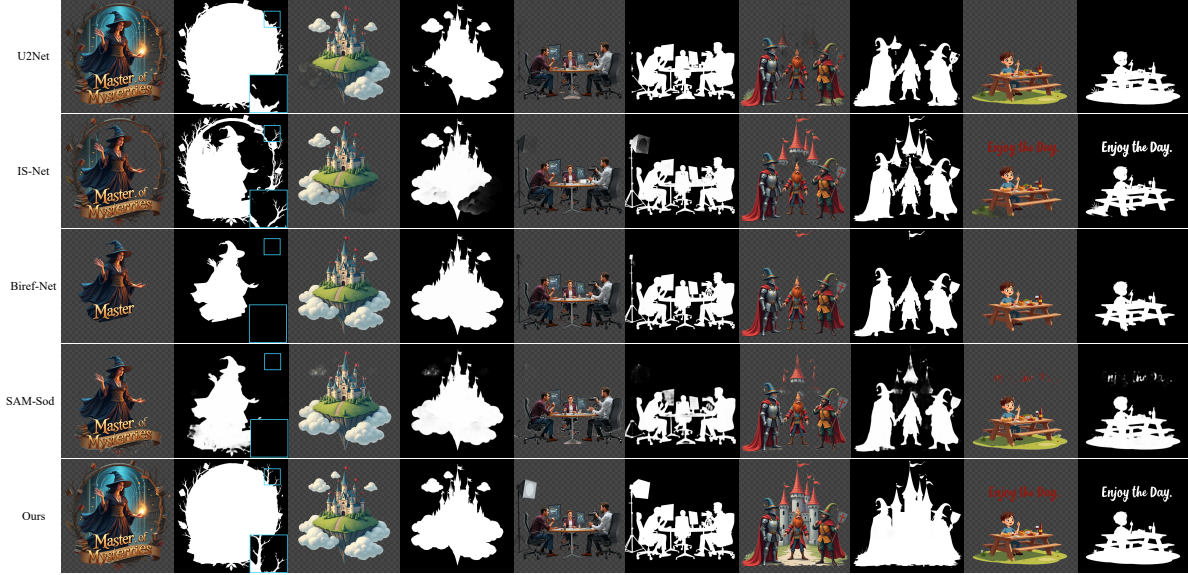
Input: Keywords K

Output: Prompt \hat{P} and Foreground Keywords \hat{n}_{fg}

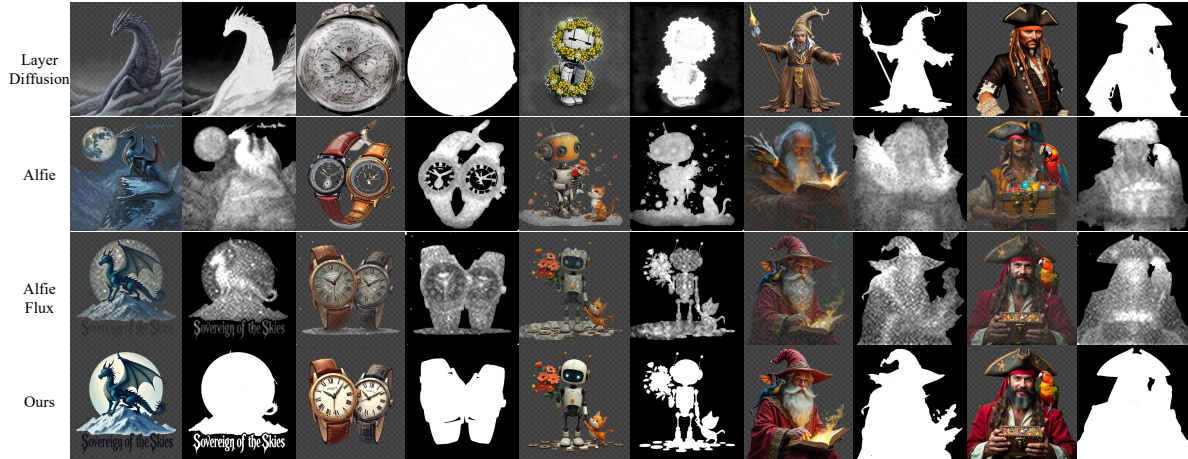
- 1: Initialize Expander, Optimizer, Extractor, Filter: $M_{exp}, M_{opt}, M_{ext}, M_{flt}$
 - 2: **function** EXTENSION_AGENT(K, P)
 - 3: **if** input only have K **then**
 - 4: $P \leftarrow M_{exp}(K)$
 - 5: **end if**
 - 6: $\hat{P} \leftarrow M_{opt}(K, P)$
 - 7: **while** M_{opt} think need revision **do**
 - 8: $\hat{P} \leftarrow M_{opt}(K, \hat{P})$
 - 9: **end while**
 - 10: **return** \hat{P}
 - 11: **end function**
 - 12: **function** EXTRACTION_AGENT(K, \hat{P})
 - 13: $n_{fg} \leftarrow M_{ext}(\hat{P})$
 - 14: $\hat{n}_{fg} \leftarrow M_{flt}(\hat{P}, n_{fg})$
 - 15: **while** M_{ext} or M_{flt} think need revision **do**
 - 16: $\hat{P} \leftarrow$ EXTENSION_AGENT(K, \hat{P})
 - 17: $n_{fg} \leftarrow M_{ext}(\hat{P})$
 - 18: $\hat{n}_{fg} \leftarrow M_{flt}(\hat{P}, n_{fg})$
 - 19: **end while**
 - 20: **return** \hat{P}, \hat{n}_{fg}
 - 21: **end function**
 - 22: $\hat{P} \leftarrow$ EXTENSION_AGENT(K)
 - 23: $\hat{P}, \hat{n}_{fg} \leftarrow$ EXTRACTION_AGENT(K, \hat{P})
 - 24: **return** \hat{P}, \hat{n}_{fg}
-

In the Extension Agent, given input K , M_{exp} expands K into more expressive prompt P . To ensure the quality of prompt P , we introduce the self-reflection in prompt generation. The optimizer M_{opt} continuously iteratively optimizes P based on K until the M_{opt} determines that the optimized prompt is good enough and finally outputs \hat{P} .

After getting the optimized prompt \hat{P} , in the Extraction Agent, the extractor M_{ext} checks M_{opt} 's output and extracts nouns $n_{fg} = [n_1, \dots, n_{\hat{N}}]$. To filter out abstract terms that could misalign the attention map and affect alpha estimation, we apply a re-extract strategy: the filter



(a) Direct comparison with generation-then-segmentation methods.



(b) Comparison with RGBA generation methods. Images are generated with the same prompt..

Figure 4. Comparison with two pipelines: generation then segmentation/matting and RGBA image generation. Our method offers high-quality and precise generation of primary subject, outperforming other methods.

M_{flt} removes abstract words like “colorful”, “details”, “data”, etc. and outputs filtered primary elements’ vocabulary $\hat{n}_{fg} = [\hat{n}_1, \dots, \hat{n}_N]$. The Extraction Agent can send a revision request to the Extension Agent if M_{ext} or M_{flt} thinks that \hat{P} or n_{fg} has too many abstract elements, the Extension Agent is required to re-provide the prompt \hat{P} to ensure the overall generation quality of the subject segmentation and the generated image.

4. Experiments

4.1. Implementation Details

In our experiments, we employed the current state-of-the-art text-to-image model, FLUX [19]. As illustrated in

Sec. 3.3, these two types of DiT blocks produce attention maps in the same manner, we treated them identically during the feature extraction process. During inference, we applied Euler Distance Sampling, and the denoising steps were set to 30. Following [37] setup, we used thresholds of 0.8, 0.2, and 0.1 to transform the attention map into a 4-value map: sure foreground, probable foreground, probable background, and sure background, ultimately using Grab-Cut to predict the mask of primary subject. In the agent framework, we use gpt-3.5-turbo[29] as the large language model. In gpt-3.5-turbo, temperature is 0.3, top p is 1, max tokens is 512.

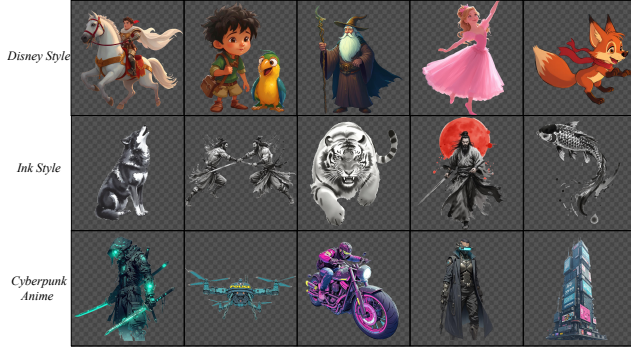


Figure 5. Results generated from our generation framework with different LoRA styles.

4.2. Qualitative Results

We conducted comprehensive qualitative and quantitative experiments to evaluate our method. We first performed comparative experiments using two different pipelines: generation-then segmentation/matting and direct RGBA generation.

For the first pipeline, we used FLUX to generate images and then applied state-of-the-art matting methods, including U2Net [34], ISNet [36], and BiRefNet [55]. Additionally, we tested salient object detection methods like SAM-SOD [12]. It is worth mentioning that the pipeline most similar to our method follows a 'generation-then-salient-object-detection' approach. Both aim to segment the most prominent subject in an image. Matting methods are trained to distinguish between the foreground and background, while segmentation methods focus on isolating the most salient object. However, both struggle to precisely delineate primary elements and retain complete information. As shown in Fig. 4a, they erroneously remove essential text content due to the absence of text guidance, such as castle in the first column and cloud in the second column. In contrast, our approach, embedded in the flux attention layers, effectively captures high-response regions of key elements in text prompt during the generation process, thereby accurately identifying key elements and maximizing the preservation of complete information.

For the second pipeline, we compared our method with LayerDiffusion[51] and Alfie[37]. For a fair comparison, we also adapt Alfie in the Flux model, see Alfie-Flux in Fig. 4b. It is important to note that we employed a zero-shot approach and did not train our model on a semi-transparent dataset. As a result, our method cannot handle semi-transparent objects in the same way as LayerDiffusion [51]. In our experiments, for a fair comparison, the prompts are kept consistent across all methods. According to the illustration in Fig. 4b, it is evident that Layer Diffusion, which necessitates comprehensive training procedures, encounters difficulties when adjusting to the most recent ad-

Table 1. Clip-Score between generated primary elements and prompt for 4 image generation methods.

	Score	Layer-Diff	Alfie	Alfie-Flux	Ours
CLIP-Score		24.92	30.78	30.88	31.73

vancements in text-to-image model technologies. As a consequence, it generally produces images with only standard quality levels, without reaching superior outcomes. The Alfie and Alfie-Flux methods, while capable of making reasonable predictions of the alpha channel, exhibit limitations in their clarity. Additionally, these methods do not accurately capture details of primary elements, affecting image clarity. However, our method can generate images that align with the provided text and retain semantically relevant details.

To validate the diversity of our generation framework, we also test the Flux model with three LoRAs[16]: dsney style¹, ink style² and cyerpunk anime style³. The results are shown in Fig. 5 Our method consistently exhibited robust performance and successfully achieved the desired effects across all LoRA integrations, demonstrating its adaptability and effectiveness.

4.3. Quantitative Results

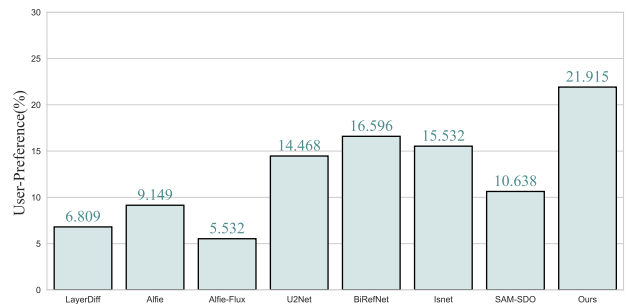


Figure 6. User preference. We compare RGBA image generation methods using the same prompts and evaluate matting methods using the same generated images.

To quantitatively evaluate our method, we first calculate the CLIP-Score (see Tab. 1). The results demonstrate that our approach achieves superior text-image alignment compared to other generation methods. Additionally, we conducted a user study in which we randomly generated 20 sets of images and recruited 30 participants. Each participant was asked to compare our method with all possible

¹Disney lora link: <https://huggingface.co/XLabs-AI/flux-lora-collection>

²Ink lora link: <https://civitai.com/models/73305/zyd232s-ink-style>

³Cyberpunk lora link: <https://civitai.com/models/128568/cyberpunk-anime-style>

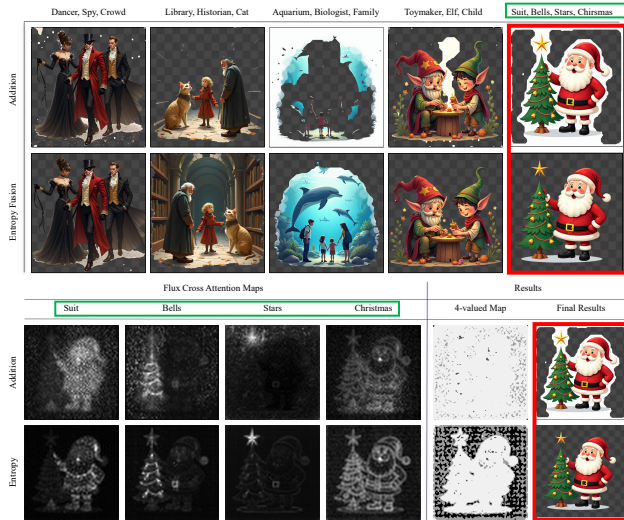


Figure 7. Comparison between two different feature fusion strategies: Addition and Entropy Fusion. The first image illustrates the final results of these two fusion methods, while the second image presents the cross-attention map corresponding to each word. Both experiments demonstrate that our entropy-based fusion method significantly enhances the generation of primary subjects.

pipelines and rank the generated images from best to worst based on their visual appeal and effectiveness. This study provided a direct assessment of the overall quality of the images produced by each approach. In our scoring system, the highest-ranked method received 8 points, while the lowest-ranked received 1 point. We then summed the scores for each method and normalized them by dividing by the total score, yielding the final user preference distribution.

As illustrated in Fig. 6, our method outperforms other RGBA generation approaches. This advantage can be attributed not only to its subject-centric generation capability but also to the strong generation ability of FLUX. Furthermore, when compared to the generation-then-matting pipeline using the same generated image, our method still achieves superior results. This is because it retains knowledge of the generation process, allowing it to better preserve the integrity of the main subject in the image.

4.4. Ablation Study

Entropy Based Feature Fusion. As shown in Fig. 7, we demonstrate the results generated using two different attention fusion methods: the entropy-based fusion and the standard addition fusion. We first present the final generation results obtained using two methods (see the first figure in Fig. 7). Then, we illustrate the attention map throughout the generation process of the last column image (see the second figure in Fig. 7). The same image is highlighted with a red rectangle, while the same prompt is indicated with a green rectangle.

The addition-based fusion strategy for blending $\mathcal{A}_C^{t,l}$ into \mathcal{A}_C provides a coarse generation of primary elements. This approach ignores the noise-to-information ratio of attention maps across different steps, leading to incomplete background removal (partial white areas in the first column) and the unintended removal of expected foreground elements (removal of the 'Library' foreground in the fourth column). The entropy-based fusion method addresses this issue by assigning higher weights to attention maps with greater information content, ensuring the accurate generation of foreground content without unexpected removal or retention.

Agent-based prompt extension and keyword extraction. In Fig. 8, we first demonstrate the effects of generating images with and without the use of an extension. Specifically, for a set of elements, we uses these elements directly as prompts to generate images when no extension is applied. As shown in Fig. 8a, images produced in this manner typically lack detail or are blurry. Conversely, when an extension is applied, the Extension agent enhances the descriptions of the elements, resulting in images with richer details. In the Fig. 8b, we illustrate the impact of using an Extraction agent to identify foreground vocabulary on subject-centric image generation. Specifically, for a given prompt, without extraction, we eliminate some generic nouns for attention indexing. In contrast, with extraction, the Extraction agent identifies foreground-related vocabulary for attention indexing. As demonstrated in Fig. 8b, without the use of an extraction agent, the generation of primary subject is suboptimal influenced by generic nouns not listed in the exclusion list. With the use of an extraction agent, we achieve more plausible generation of primary elements.

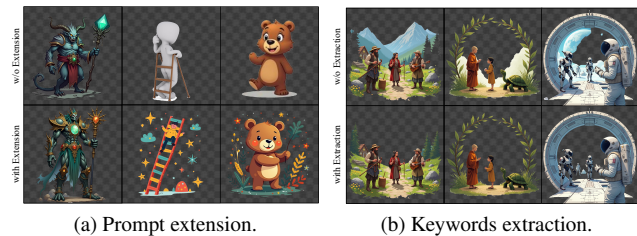


Figure 8. This figure illustrates the effects of prompt extension (a) on RGB image generation and the impact of keyword extraction (b) on mask prediction of primary subjects.

5. Conclusion

We propose a zero-shot generation pipeline capable of producing high-quality subject-centric images that seamlessly integrate with other visual content without requiring additional training. Our approach is built on two key components: an agent framework and an entropy-based attention map fusion module. Extensive qualitative and quanti-

tative experiments validate the effectiveness of our method and the functionality of its design modules. In summary, this work introduces a novel approach to generating high-quality subject-centric content, ensuring that only the desired elements are produced while eliminating unwanted content.

References

- [1] Stability AI. stable-diffusion-3-medium. <https://huggingface.co/stabilityai/stable-diffusion-3-medium>, 2024. Accessed: 2024-11-03. 4
- [2] Stability AI. stabilityai/stable-diffusion-3.5-large. <https://huggingface.co/stabilityai/stable-diffusion-3.5-large>, 2024. Accessed: 2024-11-03. 4
- [3] Michael S Albergo and Eric Vanden-Eijnden. Building normalizing flows with stochastic interpolants. *arXiv preprint arXiv:2209.15571*, 2022. 3
- [4] Ali Borji, Ming-Ming Cheng, Qibin Hou, Huaizu Jiang, and Jia Li. Salient object detection: A survey. *Computational visual media*, 5:117–150, 2019. 2
- [5] Stephen Brade, Bryan Wang, Mauricio Sousa, Sageev Oore, and Tovi Grossman. Promptify: Text-to-image generation through interactive prompt exploration with large language models. In *Proceedings of the 36th Annual ACM Symposium on User Interface Software and Technology*, pages 1–14, 2023. 3
- [6] Mingdeng Cao, Xintao Wang, Zhongang Qi, Ying Shan, Xiaohu Qie, and Yinqiang Zheng. Masactrl: Tuning-free mutual self-attention control for consistent image synthesis and editing. In *Proceedings of the IEEE/CVF International Conference on Computer Vision*, pages 22560–22570, 2023. 2, 3
- [7] Junsong Chen, Jincheng YU, Chongjian GE, Lewei Yao, Enze Xie, Zhongdao Wang, James Kwok, Ping Luo, Huchuan Lu, and Zhenguo Li. Pixart- α : Fast training of diffusion transformer for photorealistic text-to-image synthesis. In *The Twelfth International Conference on Learning Representations*, 2024. 2, 4
- [8] Xi Chen, Lianghua Huang, Yu Liu, Yujun Shen, Deli Zhao, and Hengshuang Zhao. Anydoor: Zero-shot object-level image customization. In *Proceedings of the IEEE/CVF conference on computer vision and pattern recognition*, pages 6593–6602, 2024. 1
- [9] Guillaume Couairon, Jakob Verbeek, Holger Schwenk, and Matthieu Cord. Diffedit: Diffusion-based semantic image editing with mask guidance. In *The Eleventh International Conference on Learning Representations*, 2023. 2, 3
- [10] Katherine Crowson, Stefan Andreas Baumann, Alex Birch, Tanishq Mathew Abraham, Daniel Z Kaplan, and Enrico Shippole. Scalable high-resolution pixel-space image synthesis with hourglass diffusion transformers. In *Forty-first International Conference on Machine Learning*, 2024. 3
- [11] Patrick Esser, Sumith Kulal, Andreas Blattmann, Rahim Entezari, Jonas Müller, Harry Saini, Yam Levi, Dominik Lorenz, Axel Sauer, Frederic Boesel, et al. Scaling rectified flow transformers for high-resolution image synthesis, march 2024. URL <http://arxiv.org/abs/2403.03206>. 2, 4
- [12] Shixuan Gao, Pingping Zhang, Tianyu Yan, and Huchuan Lu. Multi-scale and detail-enhanced segment anything model for salient object detection. In *Proceedings of the 32nd ACM International Conference on Multimedia*, pages 9894–9903, 2024. 2, 3, 7
- [13] Amir Hertz, Ron Mokady, Jay Tenenbaum, Kfir Aberman, Yael Pritch, and Daniel Cohen-or. Prompt-to-prompt image editing with cross-attention control. In *The Eleventh International Conference on Learning Representations*, 2023. 2, 3
- [14] Amir Hertz, Ron Mokady, Jay Tenenbaum, Kfir Aberman, Yael Pritch, and Daniel Cohen-or. Prompt-to-prompt image editing with cross-attention control. In *The Eleventh International Conference on Learning Representations*, 2023. 3
- [15] Jonathan Ho, Ajay Jain, and Pieter Abbeel. Denoising diffusion probabilistic models. In *Advances in neural information processing systems*, pages 6840–6851, 2020. 3
- [16] Edward J Hu, Yelong Shen, Phillip Wallis, Zeyuan Allen-Zhu, Yuanzhi Li, Shean Wang, Lu Wang, Weizhu Chen, et al. Lora: Low-rank adaptation of large language models. *ICLR*, 1(2):3, 2022. 7
- [17] Binyuan Huang, Yuqing Wen, Yucheng Zhao, Yaosi Hu, Yingfei Liu, Fan Jia, Weixin Mao, Tiancai Wang, Chi Zhang, Chang Wen Chen, et al. Subjectdrive: Scaling generative data in autonomous driving via subject control. *arXiv preprint arXiv:2403.19438*, 2024. 1
- [18] Alexander Kirillov, Eric Mintun, Nikhila Ravi, Hanzi Mao, Chloe Rolland, Laura Gustafson, Tete Xiao, Spencer Whitehead, Alexander C Berg, Wan-Yen Lo, et al. Segment anything. In *Proceedings of the IEEE/CVF International Conference on Computer Vision*, pages 4015–4026, 2023. 2, 3
- [19] Black Forest Labs. Flux.1 [dev] model card, flux.1-dev. <https://huggingface.co/black-forest-labs/FLUX.1-dev>, 2024. Accessed: 2024-11-03. 2, 3, 4, 6
- [20] Pengzhi Li, Qinxuan Huang, Yikang Ding, and Zhiheng Li. Layerdiffusion: Layered controlled image editing with diffusion models. In *SIGGRAPH Asia 2023 Technical Communications*, pages 1–4, 2023. 3
- [21] Yaron Lipman, Ricky TQ Chen, Heli Ben-Hamu, Maximilian Nickel, and Matt Le. Flow matching for generative modeling. *arXiv preprint arXiv:2210.02747*, 2022. 4
- [22] Bingyan Liu, Chengyu Wang, Tingfeng Cao, Kui Jia, and Jun Huang. Towards understanding cross and self-attention in stable diffusion for text-guided image editing. In *Proceedings of the IEEE/CVF Conference on Computer Vision and Pattern Recognition*, pages 7817–7826, 2024. 3
- [23] Vivian Liu and Lydia B Chilton. Design guidelines for prompt engineering text-to-image generative models. In *Proceedings of the 2022 CHI conference on human factors in computing systems*, pages 1–23, 2022. 3
- [24] Vivian Liu, Jo Vermeulen, George Fitzmaurice, and Justin Matejka. 3dall-e: Integrating text-to-image ai in 3d design workflows. In *Proceedings of the 2023 ACM designing interactive systems conference*, pages 1955–1977, 2023. 3

- [25] Xingchao Liu, Chengyue Gong, and Qiang Liu. Flow straight and fast: Learning to generate and transfer data with rectified flow. *arXiv preprint arXiv:2209.03003*, 2022. 3
- [26] Zhiheng Liu, Yifei Zhang, Yujun Shen, Kecheng Zheng, Kai Zhu, Ruili Feng, Yu Liu, Deli Zhao, Jingren Zhou, and Yang Cao. Customizable image synthesis with multiple subjects. *Advances in neural information processing systems*, 36:57500–57519, 2023. 1
- [27] Chong Mou, Xintao Wang, Liangbin Xie, Yanze Wu, Jian Zhang, Zhongang Qi, and Ying Shan. T2i-adapter: Learning adapters to dig out more controllable ability for text-to-image diffusion models. In *Proceedings of the AAAI Conference on Artificial Intelligence*, pages 4296–4304, 2024. 3
- [28] Alexander Quinn Nichol and Prafulla Dhariwal. Improved denoising diffusion probabilistic models. In *International conference on machine learning*, pages 8162–8171, 2021. 3
- [29] OpenAI. Chatgpt 3.5. <https://chatgpt.com/>, 2023. Accessed: 2024-11-03. 6
- [30] William Peebles and Saining Xie. Scalable diffusion models with transformers, 2023. 4
- [31] William Peebles and Saining Xie. Scalable diffusion models with transformers. In *Proceedings of the IEEE/CVF International Conference on Computer Vision*, pages 4195–4205, 2023. 3
- [32] PIKA. Pika. <https://pika.art/login>, 2024. Accessed: 2025-02-27. 2
- [33] Dustin Podell, Zion English, Kyle Lacey, Andreas Blattmann, Tim Dockhorn, Jonas Müller, Joe Penna, and Robin Rombach. Sdxl: Improving latent diffusion models for high-resolution image synthesis. In *The Twelfth International Conference on Learning Representations*, 2024. 2, 3, 4
- [34] Xuebin Qin, Zichen Zhang, Chenyang Huang, Masood Dehghan, Osmar R Zaiane, and Martin Jagersand. U2-net: Going deeper with nested u-structure for salient object detection. *Pattern recognition*, 106:107404, 2020. 7
- [35] Xuebin Qin, Hang Dai, Xiaobin Hu, Deng-Ping Fan, Ling Shao, and Luc Van Gool. Highly accurate dichotomous image segmentation. In *European Conference on Computer Vision*, pages 38–56. Springer, 2022. 2
- [36] Xuebin Qin, Hang Dai, Xiaobin Hu, Deng-Ping Fan, Ling Shao, and Luc Van Gool. Highly accurate dichotomous image segmentation. In *European Conference on Computer Vision*, pages 38–56. Springer, 2022. 3, 7
- [37] Fabio Quattrini, Vittorio Pippi, Silvia Cascianelli, and Rita Cucchiara. Alfie: Democratizing rgba image generation with no \$\$\$\$. *arXiv preprint arXiv:2408.14826*, 2024. 2, 3, 4, 6, 7
- [38] Robin Rombach, Andreas Blattmann, Dominik Lorenz, Patrick Esser, and Björn Ommer. High-resolution image synthesis with latent diffusion models, 2022. 2, 3, 4
- [39] Carsten Rother, Vladimir Kolmogorov, and Andrew Blake. ”grabcut”: interactive foreground extraction using iterated graph cuts. *ACM transactions on graphics (TOG)*, 23(3): 309–314, 2004. 5
- [40] Chitwan Saharia, William Chan, Saurabh Saxena, Lala Li, Jay Whang, Emily Denton, Seyed Kamyar Seyed Ghasemipour, Burcu Karagol Ayan, S. Sara Mahdavi, Rapha Gontijo Lopes, Tim Salimans, Jonathan Ho, David J Fleet, and Mohammad Norouzi. Photorealistic text-to-image diffusion models with deep language understanding, 2022. 2
- [41] Vishnu Sarukkai, Linden Li, Arden Ma, Christopher Ré, and Kayvon Fatahalian. Collage diffusion. In *Proceedings of the IEEE/CVF winter conference on applications of computer vision*, pages 4208–4217, 2024. 1
- [42] Noah Shinn, Federico Cassano, Ashwin Gopinath, Karthik Narasimhan, and Shunyu Yao. Reflexion: Language agents with verbal reinforcement learning. *Advances in Neural Information Processing Systems*, 36, 2024. 5
- [43] Jascha Sohl-Dickstein, Eric Weiss, Niru Maheswaranathan, and Surya Ganguli. Deep unsupervised learning using nonequilibrium thermodynamics. In *International conference on machine learning*, pages 2256–2265, 2015. 3
- [44] Jiaming Song, Chenlin Meng, and Stefano Ermon. Denoising diffusion implicit models. In *International Conference on Learning Representations*, 2021. 3
- [45] Raphael Tang, Linqing Liu, Akshat Pandey, Zhiying Jiang, Gefei Yang, Karun Kumar, Pontus Stenetorp, Jimmy Lin, and Ferhan Ture. What the daam: Interpreting stable diffusion using cross attention. *arXiv preprint arXiv:2210.04885*, 2022. 2, 4
- [46] Omost Team. Omost github page. <https://github.com/lllyasviel/Omost>, 2024. Accessed: 2024-11-06. 3
- [47] Narek Tumanyan, Michal Geyer, Shai Bagon, and Tali Dekel. Plug-and-play diffusion features for text-driven image-to-image translation. In *Proceedings of the IEEE/CVF Conference on Computer Vision and Pattern Recognition*, pages 1921–1930, 2023. 2, 3
- [48] vidu. vidu. <https://www.vidu.com/>, 2024. Accessed: 2025-02-27. 2
- [49] Zhao Wang, Aoxue Li, Lingting Zhu, Yong Guo, Qi Dou, and Zhenguo Li. Customvideo: Customizing text-to-video generation with multiple subjects. *arXiv preprint arXiv:2401.09962*, 2024. 1
- [50] Jingfeng Yao, Xinggang Wang, Shusheng Yang, and Baoyuan Wang. Vitmatte: Boosting image matting with pre-trained plain vision transformers. *Information Fusion*, 103: 102091, 2024. 3
- [51] Lvmin Zhang and Maneesh Agrawala. Transparent image layer diffusion using latent transparency. *arXiv preprint arXiv:2402.17113*, 2024. 2, 7
- [52] Lvmin Zhang, Anyi Rao, and Maneesh Agrawala. Adding conditional control to text-to-image diffusion models. In *Proceedings of the IEEE/CVF International Conference on Computer Vision*, pages 3836–3847, 2023. 3
- [53] Yuxuan Zhang, Yiren Song, Jiaming Liu, Rui Wang, Jinpeng Yu, Hao Tang, Huaxia Li, Xu Tang, Yao Hu, Han Pan, et al. Ssr-encoder: Encoding selective subject representation for subject-driven generation. In *Proceedings of the IEEE/CVF Conference on Computer Vision and Pattern Recognition*, pages 8069–8078, 2024. 1
- [54] Peng Zheng, Dehong Gao, Deng-Ping Fan, Li Liu, Jorma Laaksonen, Wanli Ouyang, and Nicu Sebe. Bilateral reference for high-resolution dichotomous image segmentation. *arXiv preprint arXiv:2401.03407*, 2024. 2

- [55] Peng Zheng, Dehong Gao, Deng-Ping Fan, Li Liu, Jorma Laaksonen, Wanli Ouyang, and Nicu Sebe. Bilateral reference for high-resolution dichotomous image segmentation. *arXiv preprint arXiv:2401.03407*, 2024. 7